

## Temporal force fluctuations measured by tracking individual particles in granular materials under shear

Eric I. Corwin, Eric T. Hoke, Heinrich M. Jaeger, and Sidney R. Nagel

*James Franck Institute, Department of Physics, The University of Chicago, Chicago, Illinois 60637, USA*

(Received 7 August 2007; revised manuscript received 2 May 2008; published 27 June 2008)

The network of forces between contacts in a granular material determines the response of the material to an external perturbation. As the shear stress is increased, a static, rigid material can start to yield and flow as it becomes unjammed. The time- and ensemble-averaged distribution of forces shows a marked change in character at this jamming-unjamming transition. Here, we investigate the temporal fluctuations of the forces between individual particles and the external boundary in a dense, slowly sheared system. We find that the fluctuations occur over a very broad range of time scales, resulting in power spectra characterized by a  $1/f$ -type shape and a rollover to  $1/f^2$  behavior above a turnover frequency  $f^*$ . At very low frequencies additional enhancements over the  $1/f$  contributions are observed in regions of significant in-plane shear. Moreover, the magnitude of the force fluctuation spectra produced by one particle is different from those produced by its neighbors. Such heterogeneities persist over periods of time exceeding our measurement interval (60 h). In this respect they are reminiscent of the dynamic heterogeneities that occur in liquids supercooled toward the glass transition temperature.

DOI: [10.1103/PhysRevE.77.061308](https://doi.org/10.1103/PhysRevE.77.061308)

PACS number(s): 45.70.-n, 74.40.+k, 71.55.Jv, 47.57.Gc

Granular material is precariously perched on the threshold between two very different kinds of behavior—depending on the nature of the force network between its constituent particles, a granular material can either maintain its rigidity and withstand shearing forces like a solid or yield to the shear and flow as if it were a fluid [1]. What are the differences in the force networks between the rigid and the flowing states that allow such a dramatic change in material properties as the system unjams [2,3]? We have previously shown that in the flowing, or sheared, regime the distribution of contact forces between particles and the wall can be modeled as an equilibrium system with an effective temperature, whereas in the static, rigid, solid the force-magnitude distributions are those of an out-of-equilibrium system [4]. These measurements considered ensemble- and time-averaged distributions. In the present paper, we study how the contact force of a single particle fluctuates over time as the granular material is sheared. We find that these local fluctuations have an extremely broad distribution of time scales. Moreover, when we measure the fluctuations of seemingly identical neighboring particles, we find large differences in the intensity of the fluctuations over the course of our longest measurement interval (60 h). This result is surprising, since the particles are all in the same environment undergoing shear, and is reminiscent of the dynamic heterogeneities that appear in glasses near the glass transition.

The time- and ensemble-averaged distribution of contact forces has been investigated extensively for static, un-sheared, granular media [5–18]. By contrast, the temporal variations of contact forces and impulses in sheared material have been studied in only a few situations by experiment [18–20] and simulation [21]. Experiments in two-dimensional (2D) systems tracked individual particles. Experiments in 3D systems used a fixed force transducer mounted flush with the container wall; when beads traveled over the transducer surface the measurements recorded the net force or impulse of all particles in contact with it at a

given time which, depending on the transducer area and bead size, could be hundreds of beads. The resultant data therefore were a convolution of the force fluctuations of many beads with the step function of each bead entering and exiting the measurement surface. Our experiments use a different approach that tracks the motion of single particles at the bounding surface of 3D systems and records the individual contact force variations locally.

In order to measure force fluctuations occurring on a single particle, we use the same shear cell, shown schematically in Fig. 1, as was used to measure the time-averaged distribution of contact forces between particles and the bottom plate [4]. Particles are sheared by rotating the roughened plunger at the top surface at fixed angular velocity  $\omega = 2\pi f_{\text{drive}}$ . This plunger is maintained at constant vertical pressure by loading it with a stiff spring (monitored by another force transducer). Because the bottom and sidewalls of this shear cell are stationary, the rotating plunger results in a complex shear flow profile where particles are retarded by friction with the side and bottom but nevertheless can slip along those surfaces. Granular material, consisting of  $3.06 \pm 0.04$  mm diameter soda lime glass beads, is confined in a cylinder of radius  $R = 6.5$  cm and filled to a height of approximately  $H = 4.5$  cm (15 bead diameters). For the experiments reported here, the plunger at the top surface rotates at a frequency  $f_{\text{drive}} = 0.18$  Hz and applies a compressive force of 1380 N, chosen to bring the average force on each bead into a range appropriate for easy detection and measurement.

The contact forces in the normal direction applied by each individual bead on the bottom plate are detected using a photoelastic force transducer covering the whole bottom surface of the cylinder. This force transducer consists of a thin layer of photoelastic polymer (Vishay Micro-Measurements, Raleigh, NC, thickness 0.25 mm, hardness 80 Durometer), mirrored on its top surface and bonded to a 9.5-mm-thick clear glass plate for mechanical support. The position and

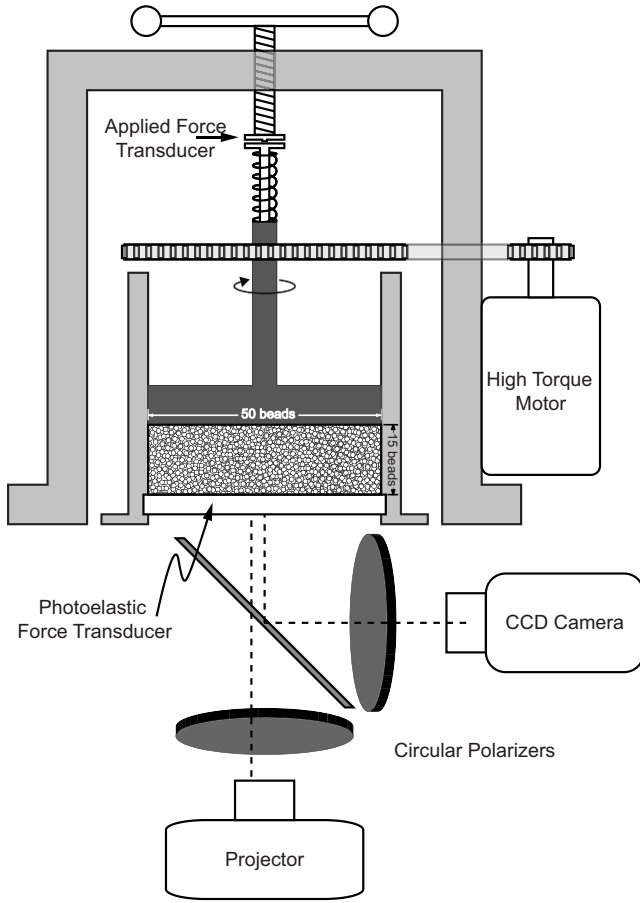


FIG. 1. Schematic diagram of the force-fluctuation measurement apparatus.

magnitude of the force from each individual particle can be measured by imaging this plate through an analyzer oriented to block unrotated light so that local contact forces appear as bright spots. For tracking and analysis of these spots the image resolution is chosen to have a minimum of  $4 \times 4$  pixels per spot. In order to determine the force magnitudes, the local brightness is calibrated everywhere on the bottom surface against a known applied force. This is achieved by analyzing the data from a slowly rotating monolayer of beads, compressed against the bottom by a soft rubber sheet sandwiched between the beads and the plunger. To obtain the temporal fluctuations over a broad dynamic range, we videotape our force transducer at rates from 0.1 to 3000 frames/s and over intervals ranging from 1 s to 60 h. High frame rates are obtained using a Phantom V7, and mid and low frame rates are obtained with a Sony DCR-VX2000 digital video camera. Upon taking the Fourier transform of these data, this results in a usable frequency range covering eight orders of magnitude from  $f=10^{-5}$  to  $10^3$  Hz.

Our apparatus also allows us to measure the velocity profile at the bottom and side boundaries. Since the confining cylinder is transparent, we can measure the azimuthal velocity  $V_\theta(z)$  of the particles traveling along the sidewalls as a function of depth from the top surface,  $z$ . Figure 2(a) shows that the azimuthal velocity  $V_\theta$  as a function of depth decays exponentially. Therefore the vertical shear strain rate

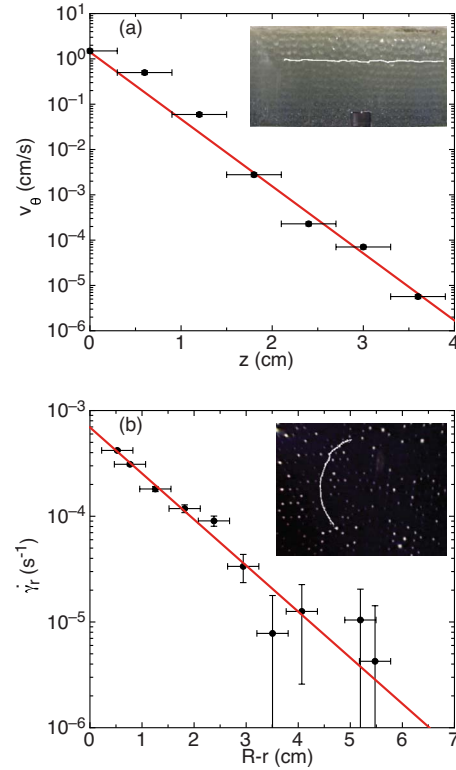


FIG. 2. (Color online) (a) Azimuthal velocity  $V_\theta$  at the outer wall as a function of depth below the surface  $z$ . (b) Radial shear strain rate  $\dot{\gamma}_r$  measured along the bottom plate of the system as a function of distance from the wall,  $R-r$ . Lines are fits to the data. Insets show representative traces of a single particle moving for 2 min along the sidewall (a) and for 20 min along the bottom plate (b), superimposed on snapshots of the whole field of view.

at the confining side wall,  $\dot{\gamma}_z = dV_\theta/dz$ , decays exponentially as  $\dot{\gamma}_z = \dot{\gamma}_{z_0} \exp(-z/z_0)$  with a characteristic length  $z_0 = 2.93 \pm 0.26$  mm (i.e., approximately 1 bead diameter) and prefactor  $\dot{\gamma}_{z_0} = f_{\text{drive}} 2\pi R/z_0 = 4.0$  s $^{-1}$ . This is in agreement with the results of Ref. [22], albeit with a slightly faster decay, presumably because of additional shear caused by the wall friction. At the bottom surface, we measure the local angular velocity  $\omega(r)$  as a function of radius  $r$  by tracking the motion of beads as imaged by the force transducer and compute the radial shear strain rate  $\dot{\gamma}_r = r d\omega(r)/dr$ . This is shown in Fig. 2(b). We find that the sidewalls introduce a radial shear which also decays exponentially with distance from the sidewalls,  $\dot{\gamma}_r = \dot{\gamma}_{r_0} \exp[-(R-r)/r_0]$  with a characteristic length  $r_0 = 9.5 \pm 1.3$  mm ( $\sim 3$  bead diameters) and prefactor  $\dot{\gamma}_{r_0} = 6 \times 10^{-4}$  s $^{-1}$ . Further, since the photoelastic polymer that makes up the bottom surface is relatively smooth, we find that there is significant slip present between the beads and the bottom surface, such that  $\omega(r)$  does not equal zero even in the region in which  $\dot{\gamma}_r$  is zero.

Figure 3(a) shows a representative time series of the recorded force fluctuations on the bottom plate by plotting the time variation of brightness for an individual bead labeled by  $j$ . There are fluctuations on every time scale as can be seen by expanding the time axis [Figs. 3(a)–3(e)]. We show this quantitatively below. As previously reported by Behringer

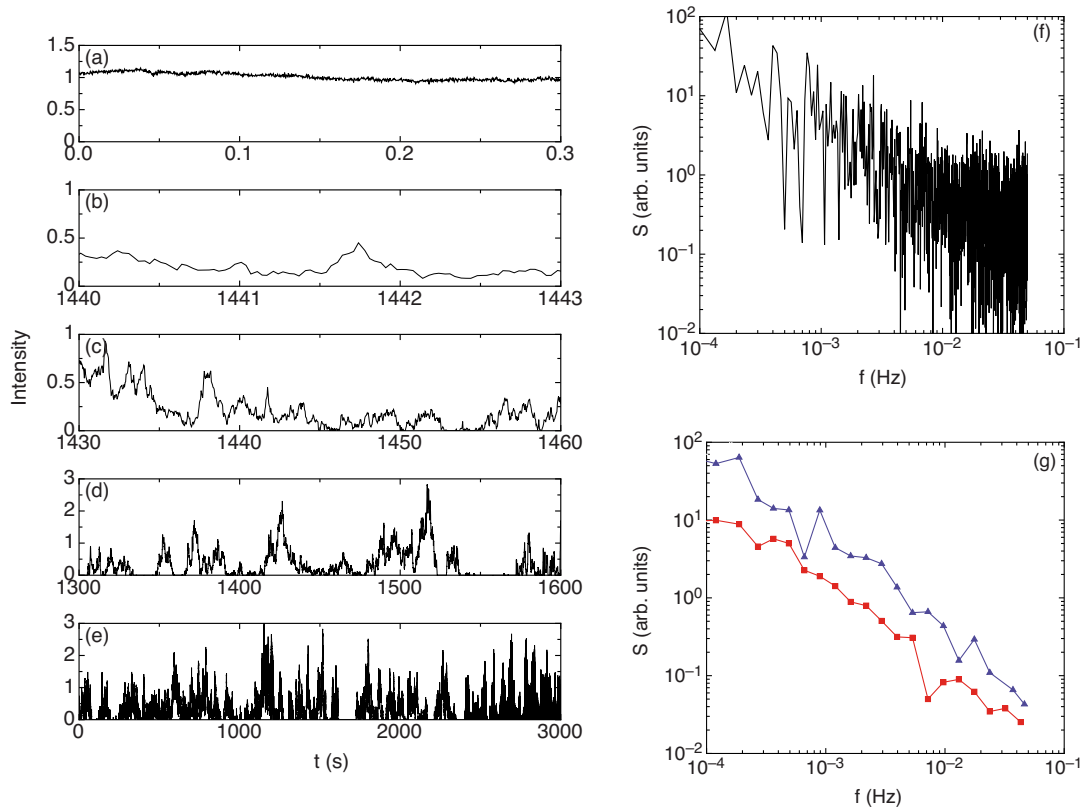


FIG. 3. (Color online) Time series of intensity and power spectra of forces exerted by individual particles at  $r=40$  mm. (a)–(e) Intensity of the brightness due to the force of a single particle over different time periods as indicated. There are fluctuations over all the time scales measured (up to 60 h). (f) Power spectrum for a single bead, calculated directly from the data in (a)–(e). No binning or averaging was performed. (g) Comparison of binned power spectra for two neighboring particles at the same distance  $r=40$  mm from the center, showing that there is heterogeneous dynamics in the system that persists over times scales that are long compared to the individual rearrangements of the beads or the driving shear rate at the top surface.

and co-workers, the fluctuations are large compared to their mean [18]. To study the nature of these fluctuations, we compute the power spectrum  $S_j(f)$  of the time trace for each tracked bead [Fig. 3(f)]. The time-averaged force on a grain is proportional to the dc value of the power spectrum. Rather than observing the  $1/f^2$  decay characteristic of a single relaxation time, we observe a much broader distribution. There is no sharp peak corresponding to a dominant shear strain rate that one might expect if, for example, the most rapid rearrangements near the top surface dominated the fluctuations in the force network.

We demonstrate that beads experiencing the same local environment exhibit significantly different fluctuation magnitudes so that even over the longest intervals studied (60 h) the time-averaged mean force varies from particle to particle. However, all beads at a given distance from the center exhibit power spectra with the same characteristic shape. In Fig. 3(g), we show  $S_j(f)$  for two neighboring beads at the same radius ( $r=40$  mm) that are measured over the same interval of  $\sim 3$  h. They were explicitly chosen to have time-averaged mean forces that were within 20% of each other over this period. During this time the grains remain neighbors and trace out circular paths that make several revolutions along the bottom plate of the system, while over the same interval the top piston makes several thousands of revolutions. During this time any small, residual variations in

forcing as a result of slight wobbles in the driving plate above or imperfections in the force transducer below would be experienced by both beads. Thus, any differences in the power spectra of the two beads must result from persistent differences in the interactions between each bead and the network of forces in the system. Over this period, as seen in Fig. 3(g), the respective power spectra of these two beads exhibit a similar frequency dependence, yet their magnitudes differ by about a factor of 4. Thus, two beads chosen to be experiencing the same local environment, compressed with nearly the same time-averaged force will undergo fluctuations in force with power spectra of differing strength. Moreover, for neighboring beads experiencing differing time-averaged forces, we find the strength of the spectra and the average force on a bead to be uncorrelated.

To obtain better statistics on the shape of the power spectra, we can determine a mean spectrum  $S_r(f)$  averaged over all the beads in an annulus at radius  $r$  centered on the axis of rotation. Each annulus has a width of 3 mm, i.e., 1 bead diameter. In each annulus, the beads all travel with the same average angular velocity and the same average strain rate. In Fig. 4 these spectra cover a frequency range  $10^{-5} < f < 10^3$  Hz, obtained by superposing the spectra computed at three sampling rates: 3 kHz, 30 Hz, and 0.1 Hz. The lengths of these runs were 1 s, 1 h, and 60 h, respectively.

The simplest shearing conditions occur near the center of

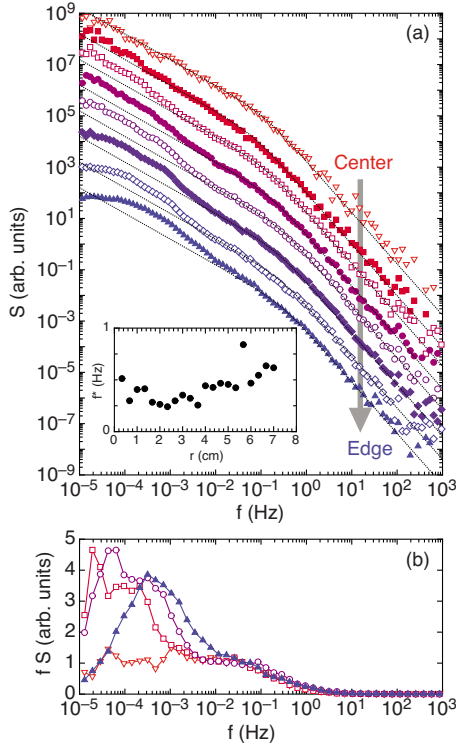


FIG. 4. (Color online) Power spectra  $S_r(f)$  averaged over all particles in an annulus at given radius  $r$ . (a) Power spectra in 3-mm-wide annuli centered at  $r=1.5, 7.5, 16.5, 22.5, 34.5, 43.5, 52.5,$  and  $61.5$  mm (top to bottom; the spectra from different annuli are offset vertically for clarity). (b)  $fS(f)$  for the same data as in (a) to show the enhancement above the  $1/f$  behavior at low frequency.

the pack,  $0 < r < 3$  mm. There the in-plane shearing is insignificant (i.e.,  $\dot{\gamma}_r=0$ ) and near the bottom the material moves as a solid plug, slowly slipping over the bottom surface. From Fig. 4 we find  $1/f$  behavior at low frequencies, rolling over to  $1/f^2$  behavior above a characteristic turnover frequency  $f^*$ . This high-frequency rollover to  $1/f^2$  behavior is similar to that seen with fixed transducer measurements in Ref. [18]. The turnover frequency is of the same order of magnitude as the shear strain rate imposed by the top plunger ( $\sim 1$  Hz). Effectively, this imposed rate sets the upper limit for frequency scales at which particle rearrangements can occur, causing the spectra to roll off as  $1/f^2$  above  $f^*$ .

It is not obvious why the system should also rearrange at time scales stretching all the way to the maximum duration of our measurements, 60 h. Evidence for  $1/f^\alpha$  behavior, with  $0 < \alpha < 2$ , at low frequencies was previously found by Behringer *et al.* in 3D experiments using a fixed transducer as well as in 2D experiments using birefringent disk packings [18,19]. In those experiments, however, the frequency span was too limited to allow for a clear identification of the power-law exponent.

For annuli farther from the center, the radial shear  $\dot{\gamma}_r$  increases as shown in Fig. 2(b). The overall shape of  $S_r(f)$  remains similar to that near  $r=0$  with a  $1/f$  region turning over to a  $1/f^2$  region above a frequency  $f^*$ . The value of  $f^*$  increases slightly with radius as shown in the inset of Fig. 4(b), and the roughly linear dependence of  $f^*$  with radius  $r$  for  $r > 5$  appears to reflect the linear increase of azimuthal

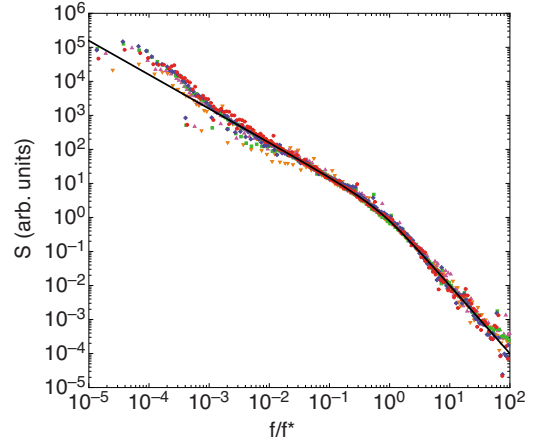


FIG. 5. (Color online) Master curve of all the power spectra. The horizontal axis has been scaled by the turnover frequency  $f^*$ . The line is a fit to Eq. (2).

velocity, and therefore shear rate, as a function of radius imposed by the plunger. Normalizing the frequency axis by the turnover frequency, all spectra can be plotted on a single master curve (Fig. 5). There is a very good collapse of the data except at the very lowest frequencies. This is in line with the finding of Ref. [18], based on experiments in which the driving frequency was varied, that the fluctuations are essentially rate independent.

The deviations from scaling seen in Fig. 5 appear to be due to a radius-dependent low-frequency enhancement to  $S_r(f)$ . As can be seen from Fig. 4, this feature moves toward higher frequency as  $r$  increases toward  $R$ , the radius of the outer wall. This enhancement can be most easily detected if we remove the  $1/f$  contribution from the data by multiplying the noise power  $S_r(f)$  by the frequency  $f$  [Fig. 4(b)]. At the center of the cell, we are not able to see any enhancement. At the largest radius, near the wall, the enhancement has a peak near  $3 \times 10^{-4}$  Hz.

The crossover from  $1/f$  to  $1/f^2$  behavior above  $f^*$  can be modeled in the standard way [23] for treating  $1/f$  noise. To model this behavior we assume that the fluctuation spectrum is the sum of individual Lorentzian processes each with a characteristic frequency  $f_c$  and a distribution of characteristic frequencies with the following form:

$$D(f_c) = \begin{cases} \xi f_c, & f_c < f^*, \\ 0, & f^* < f_c. \end{cases} \quad (1)$$

The power spectrum is the integral of all the Lorentzian contributions centered at  $f_c$ :

$$S(f) = \int_0^\infty D(f_c) \frac{f_c}{f_c^2 + f^2} df_c = \xi \int_0^\infty \frac{f_c}{f_c^2 + f^2} \arctan \frac{f^*}{f} df_c. \quad (2)$$

This produces  $1/f$  behavior at frequencies below  $f^*$  and  $1/f^2$  above  $f^*$ .

We can tentatively interpret the distribution of characteristic frequencies,  $D(f_c)$ , as due to a distribution of shear rates as a function of height. The total force exerted by a bead on the bottom plate is affected by the shearing of all the beads lying above it in the system. As shown in Fig. 2(a), at the

outer edge of the system, there is an exponentially wide distribution of shear rates in the vertical direction:  $\dot{\gamma}_z = \dot{\gamma}_{z_0} e^{z/z_0}$ . Although we cannot measure the vertical shear rate inside the pack, we assume that it follows the same functional form as seen at the edge with the same decay constant  $z_0$  but with a radius-dependent overall scale factor  $\dot{\gamma}_{z_0}(r)$ . By comparing  $\omega(r)$  measured at the bottom surface to the drive frequency at the top surface, we can deduce that  $\dot{\gamma}_{z_0}(r)$  in the center is decreased by less than an order of magnitude from the value measured at the edge of the pack.

If each layer of beads produces a characteristic frequency  $f_c$  equal to the local shear rate  $\dot{\gamma}_z$ , then one will observe a distribution of frequencies,  $D(f_c) = D(z) |dz/df_c| = z_0/f_c$ , which is the same form as Eq. (1) with  $\xi$  replaced by  $z_0$ . Within this picture the broad  $1/f$  character of temporal fluctuations arises from an exponential distribution of shear strain rates above the bottom layer. Thus, in contrast to the time- and ensemble-averaged force distributions  $P(f)$  [4–18],  $S_r(f)$  contains information about the way forces propagate through the 3D material. Although this is an appealing picture which reproduces the overall characteristics of the power spectrum shown in our data in Fig. 4, we note that it is not clear that the effect of shear from each layer can simply be integrated as was done to arrive at Eq. (2).

Because the shear rate  $\dot{\gamma}_z$  depends on depth, spectra taken over a finite duration at the bottom surface sample only the fluctuations that occur due to shear above a cutoff depth. Thus, the lowest frequency sampled sets the depth  $z$  below which fluctuations cannot be detected. For the data in Fig. 4, this lowest frequency, and thus slowest detectable shear rate, is  $10^{-5} \text{ s}^{-1}$ , corresponding to a depth of  $z \sim 31 \pm 3 \text{ mm}$ , where the error is set by our assumption that  $\dot{\gamma}_{z_0}(r)$  at the bead's radius is within an order of magnitude of the value measured at the side wall. Given the total packing height of 45 mm, this means that, over the measurement interval, the packing configuration in the bottom 3–5 layers appeared essentially frozen. While this frozen configuration then acted as a transmitter for faster force fluctuations from layers above, its own heterogeneous fabric of local contact forces was not sufficiently shuffled, preserving the different sensitivity to fluctuations that characterizes different force paths through an effectively static granular medium. If the system were measured over a time period longer than the time scale set by the shear strain rate at the bottom surface (and significantly longer than is accessible to this experiment) then neighboring beads should experience identical power spectra.

The ability to track the forces on individual beads over time allows us to probe fluctuations that are inaccessible to measurements employing fixed transducers [18–20]. At very

low frequencies, we have shown that there is an extra contribution to  $S(f)$  which increases as a function of radius. We suggest that this enhancement is due to the presence of the in-plane shearing that grows in magnitude near the sidewalls,  $\dot{\gamma}_r = \dot{\gamma}_{r_0} e^{-((R-r)/r_0)}$ . We note that  $\dot{\gamma}_{r_0} \sim 10^{-3} \text{ Hz}$ , which is approximately in the right frequency regime to match excess fluctuations shown in Fig. 4(b).

The diversity in the dynamics we find in sheared granular materials is reminiscent of the dynamical heterogeneities [24–29] that are observed in liquids as their temperature is lowered toward the glass transition temperature. In those systems, there are also heterogeneities where molecules in one region of the liquid can have abnormally slow dynamics that persist for periods that are ostensibly much longer than the average relaxation time for the liquid at that temperature. The fluctuations that we observe in the forces on individual beads likewise persist over time scales much longer than those set by the average shear strain rate throughout the system. This phenomenon is visible because we are able to view the forces exerted by multiple individual beads over a long period of time and would be washed out if the measurement were insensitive to individual particle forces [18–20]. In our granular experiments, this heterogeneity is caused by local dynamics near the bottom surface, where the forces are measured, being much slower than in regions higher in the cell. Nevertheless, the higher-frequency fluctuations—caused by shear in the upper layers—can be detected in this region.

In conclusion, we have observed the temporal force fluctuations on individual particles in a granular system as it is being sheared. Because of our wide dynamic range of eight orders of magnitude in frequency, we are able to identify features that would otherwise be difficult to detect, such as the knee in the spectrum and the excess of very low-frequency fluctuations. As in other disordered systems, such as glasses, we find a very broad distribution of time scales that produces slow, nonexponential, relaxation. In our case, we have ascribed this distribution to the very rapid variation of shear rate as a function of the depth. Likewise, the low-frequency enhancement is consistent with contributions from radial, in-plane, shearing produced by the sidewalls. A further analogy with glassy systems can be found in the heterogeneous dynamics as observed in the fluctuations: adjacent particles have very different dynamics which persist over many times the relaxation rate set by the average shear strain rate throughout the system.

We are grateful to Xiang Cheng, John Royer, and Martin van Hecke for stimulating conversations. This work was supported by NSF MRSEC Grant No. DMR-0213745 and DOE Grant No. DE-FG02-03ER46088.

- [1] H. M. Jaeger, S. R. Nagel, and R. P. Behringer, *Rev. Mod. Phys.* **68**, 1259 (1996).  
 [2] *Jamming and Rheology: Constrained Dynamics on Microscopic and Macroscopic Scales*, edited by A. J. Liu and S. R. Nagel (Taylor and Francis, London, 2001).

- [3] A. J. Liu and S. R. Nagel, *Nature (London)* **396**, 21 (1998).  
 [4] E. I. Corwin, H. M. Jaeger, and S. R. Nagel, *Nature (London)* **435**, 1075 (2005).  
 [5] C.-h. Liu, S. R. Nagel, D. A. Schecter, S. N. Coppersmith, S. Majumdar, O. Narayan, and T. A. Witten, *Science* **269**, 513

- (1995).
- [6] D. M. Mueth, H. M. Jaeger, and S. R. Nagel, *Phys. Rev. E* **57**, 3164 (1998).
- [7] G. Løvoll, K. J. Måløy, and E. G. Flekkøy, *Phys. Rev. E* **60**, 5872 (1999).
- [8] F. Radjai, S. Roux, and J. J. Moreau, *Chaos* **9**, 544 (1999).
- [9] H. A. Makse, D. L. Johnson, and L. M. Schwartz, *Phys. Rev. Lett.* **84**, 4160 (2000).
- [10] D. L. Blair, N. W. Mueggenburg, A. H. Marshall, H. M. Jaeger, and S. R. Nagel, *Phys. Rev. E* **63**, 041304 (2001).
- [11] C. S. O'Hern, S. A. Langer, A. J. Liu, and S. R. Nagel, *Phys. Rev. Lett.* **86**, 111 (2001).
- [12] L. E. Silbert, G. S. Grest, and J. W. Landry, *Phys. Rev. E* **66**, 061303 (2002).
- [13] S. F. Edwards and D. V. Grinev, *Granular Matter* **4**, 147 (2003).
- [14] C. S. O'Hern, L. E. Silbert, A. J. Liu, and S. R. Nagel, *Phys. Rev. E* **68**, 011306 (2003).
- [15] J. Brujic, S. F. Edwards, I. Hopkinson, and H. A. Makse, *Physica A* **327**, 201 (2003).
- [16] J. H. Snoeijer, T. J. H. Vlugt, M. van Hecke, and W. van Saarloos, *Phys. Rev. Lett.* **92**, 054302 (2004).
- [17] T. S. Majmudar and R. P. Behringer, *Nature (London)* **435**, 1079 (2005).
- [18] D. Howell and R. P. Behringer, in *Powders and Grains 97*, edited by R. P. Behringer and J. T. Jenkins (Balkema, Rotterdam, 1997), pp. 337–340; D. W. Howell, R. P. Behringer, and C. T. Veje, *Chaos* **9**, 559 (1999); D. Howell, R. P. Behringer, and C. Veje, *Phys. Rev. Lett.* **82**, 5241 (1999).
- [19] B. Miller, C. O'Hern, and R. P. Behringer, *Phys. Rev. Lett.* **77**, 3110 (1996).
- [20] E. Longhi, N. Easwar, and N. Menon, *Phys. Rev. Lett.* **89**, 045501 (2002).
- [21] A. Ferguson, B. Fisher, and B. Chakraborty, *Europhys. Lett.* **66**, 277 (2004).
- [22] D. M. Mueth, G. F. Debregeas, G. S. Karczmar, P. J. Eng, S. R. Nagel, and H. M. Jaeger, *Nature (London)* **406**, 385 (2000).
- [23] M. B. Weissman, *Rev. Mod. Phys.* **60**, 537 (1988).
- [24] K. Schmidt-Rohr and H. Spiess, *Phys. Rev. Lett.* **66**, 3020 (1991).
- [25] M. T. Cicerone and M. D. Ediger, *J. Chem. Phys.* **103**, 5684 (1995); E. R. Weeks and D. A. Weitz, *Phys. Rev. Lett.* **89**, 095704 (2002).
- [26] D. N. Perera and P. Harrowell, *Phys. Rev. E* **54**, 1652 (1996).
- [27] R. Yamamoto and A. Onuki, *Phys. Rev. E* **58**, 3515 (1998).
- [28] B. Doliwa and A. Heuer, *Phys. Rev. Lett.* **80**, 4915 (1998).
- [29] C. Donati, S. C. Glotzer, P. H. Poole, W. Kob, and S. J. Plimpton, *Phys. Rev. E* **60**, 3107 (1999).